DOA ESTIMATION VIA COARRAY TENSOR COMPLETION WITH MISSING SLICES

Hang Zheng[1]*, Chengwei Zhou*[1]*, André L. F. de Almeida*[2]*, Yujie Gu*[3]*, and Zhiguo Shi*[1,4]

[1] College of Information Science and Electronic Engineering, Zhejiang University, Hangzhou 310027, China
[2] Department of Teleinformatics Engineering, Federal University of Ceará, Fortaleza 60020-181, Brazil
[3] Electronics and Safety, Aptiv, Agoura Hills, CA 91301, USA
[4] International Joint Innovation Center, Zhejiang University, Haining 314400, China

ABSTRACT

In this paper, a coarray tensor completion-based direction-of-arrival (DOA) estimation method is proposed for coprime planar array. To perform Nyquist-matched coarray signal processing, the completion of the coarray tensor corresponding to an augmented discontinuous virtual array is pursued. However, it is difficult to impose a low-rank regularization on the incomplete coarray tensor with slices of missing elements for its completion. To solve this problem, a structural tensorization approach is designed to reshape the incomplete coarray tensor into one with distributed missing elements. As such, a coarray tensor completion problem based on tensor nuclear norm minimization is formulated to complete these missing elements. By exploiting the filled virtual array obtained from the completed coarray tensor, a super-resolution DOA estimation can be achieved in closed-form.

Index Terms— Coarray tensor, coprime planar array, direction-of-arrival estimation, tensor completion.

1. INTRODUCTION

Tensor-based direction-of-arrival (DOA) estimation for sparse arrays [1–6] has attracted tremendous attentions recently due to the utilization of multi-dimensional signals sampling below the Nyquist rate [7,8]. The emerging coarray tensor-based approaches push the Nyquist-matched DOA estimation towards the coprime array [9–11], which is a kind of typical sparse array with systematic design [12, 13]. However, the existing methods only consider the continuous part of the augmented virtual array for Nyquist matching, and the performance loss due to discarding the discontinuous virtual sensors cannot be compensated by tensor modeling. Therefore, it is still an important problem how to make full use of all virtual sensors for coarray tensor-based DOA estimation.

Although the virtual array interpolation techniques have been investigated for coprime linear arrays in a framework of matrix-based coarray signal processing [14–17], they cannot be applied to the multi-dimensional virtual arrays with tensorial coarray modeling. To complete tensors with randomly missing elements, the tensor completion techniques have been developed to repair corrupted images characterized by incomplete tensors [18, 19]. However, for coprime array DOA estimation, the discontinuous virtual arrays derived from the tensor statistics naturally own slices of holes [7, 20], preventing a sufficient low-rank regularization on the incomplete coarray tensor for its completion. To address this problem, in the field of image restoration, the slice completion methods based on dimensional-duplication and rank-increment are proposed to approximate the tensor decomposition representation of the image tensors with an iteratively increased rank [21,22]. Nevertheless, these methods are not applicable to DOA estimation since our derived coarray tensor owns a determined structure with a fixed rank. Therefore, it is challengeable to complete a coarray tensor with whole missing slices for DOA estimation.

In this paper, a coarray tensor completion-based two-dimensional (2-D) DOA estimation method is proposed for coprime planar array (CPA). To achieve a Nyquist-matched coarray tensor processing, it is necessary to complete the second-order coarray tensor corresponding to an augmented discontinuous virtual cubic array. However, due to the existence of whole slices of missing elements in the coarray tensor, low-rank regularization cannot be directly applied for its completion. To overcome this problem, a structural tensorization approach is designed to distribute the missing elements in the coarray tensor, such that a tensor nuclear norm minimization problem can be effectively imposed for coarray tensor completion. The completed coarray tensor corresponds to a filled virtual cubic array, ensuring the Nyquist-matched DOA estimation. As shown in our numerical results, the proposed method is superior to competing matrix-based and tensor-based methods both in accuracy and in resolution.

2. COPRIME PLANAR ARRAY TENSOR MODEL

As shown in Fig. 1, a CPA consists of a pair of sparse uniform rectangular arrays (URAs) $\mathbb{P}_i$ with $q_x^{(\mathbb{P}_i)} \times q_y^{(\mathbb{P}_i)}$ sensors, where

This work was partially supported by the National Natural Science Foundation of China (No. 61901413, U21A20456), the National Key R&D Program of China (No. 2018YFE0126300), and the Zhejiang University Education Foundation Qizhen Scholar Foundation.

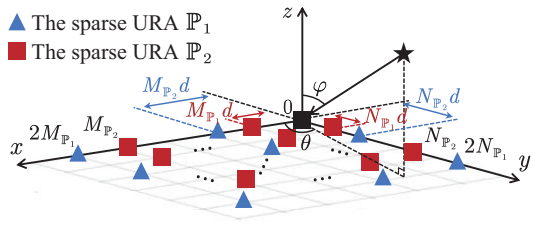

Fig. 1. The geometry of the coprime planar array.

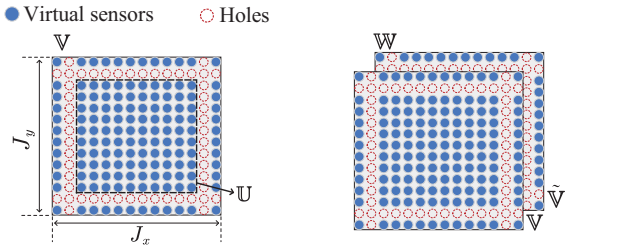

(a) Augmented virtual planar array (b) Discontinuous virtual cubic array

Fig. 2. Virtual array geometries of the coprime planar array.

$q_x^{(\mathbb{P}_i)}$ and $q_y^{(\mathbb{P}_i)}$ respectively denote the number of sensors in $\mathbb{P}_i$ along the x-axis and the y-axis, and $i \in \{1, 2\}$. Here, $q_x^{(\mathbb{P}_1)} = 2M_{\mathbb{P}_1}$, $q_y^{(\mathbb{P}_1)} = 2N_{\mathbb{P}_1}$, and $q_x^{(\mathbb{P}_2)} = M_{\mathbb{P}_2}$, $q_y^{(\mathbb{P}_2)} = N_{\mathbb{P}_2}$, where both $(M_{\mathbb{P}_1}, M_{\mathbb{P}_2})$ and $(N_{\mathbb{P}_1}, N_{\mathbb{P}_2})$ are pairs of coprime integers. The inter-element spacings for the sparse URA $\mathbb{P}_1$ are $d_x^{(\mathbb{P}_1)} = M_{\mathbb{P}_2} d$ and $d_y^{(\mathbb{P}_1)} = N_{\mathbb{P}_2} d$ along the x-axis and the y-axis, respectively, where $d = \lambda/2$, and λ is the source wavelength. Similarly, the inter-element spacings for the sparse URA $\mathbb{P}_2$ are $d_x^{(\mathbb{P}_2)} = M_{\mathbb{P}_1} d$ and $d_y^{(\mathbb{P}_2)} = N_{\mathbb{P}_1} d$. As such, the sensors of two sparse URAs only overlap at the origin position $(0, 0)$, and the total number of sensors in the CPA is $4M_{\mathbb{P}_1}N_{\mathbb{P}_1} + M_{\mathbb{P}_2}N_{\mathbb{P}_2} - 1$.

Assume that there are K uncorrelated far-field narrowband sources impinging on the CPA, where the k-th source is located at (θ_k, φ_k) with azimuth $\theta_k \in [0, \pi]$ and elevation $\varphi_k \in [-\frac{\pi}{2}, \frac{\pi}{2}]$. To preserve the original structure of the received signals, T snapshots containing 2-D spatial information are cast as T slices to formulate an additional temporal dimension. As such, the received signals of the i-th sparse URA $\mathbb{P}_i$ can be represented as a 3-D tensor $\boldsymbol{\mathcal{X}}_{\mathbb{P}_i} \in \mathbb{C}^{q_x^{(\mathbb{P}_i)} \times q_y^{(\mathbb{P}_i)} \times T}$ as

$$\boldsymbol{\mathcal{X}}_{\mathbb{P}_i} = \sum_{k=1}^{K} \boldsymbol{a}_x^{(\mathbb{P}_i)}(k) \circ \boldsymbol{a}_y^{(\mathbb{P}_i)}(k) \circ \boldsymbol{s}_k + \boldsymbol{\mathcal{N}}_{\mathbb{P}_i}, \quad (1)$$

where $\boldsymbol{a}_x^{(\mathbb{P}_i)}(k) = [1, e^{-\jmath\frac{2\pi}{\lambda} d_x^{(\mathbb{P}_i)} \mu_k}, \cdots, e^{-\jmath\frac{2\pi}{\lambda}(q_x^{(\mathbb{P}_i)}-1) d_x^{(\mathbb{P}_i)} \mu_k}]^{\mathrm{T}}$ and $\boldsymbol{a}_y^{(\mathbb{P}_i)}(k) = [1, e^{-\jmath\frac{2\pi}{\lambda} d_y^{(\mathbb{P}_i)} \nu_k}, \cdots, e^{-\jmath\frac{2\pi}{\lambda}(q_y^{(\mathbb{P}_i)}-1) d_y^{(\mathbb{P}_i)} \nu_k}]^{\mathrm{T}}$ are the steering vectors corresponding to the k-th source with $\mu_k = \sin\varphi_k \cos\theta_k$ and $\nu_k = \sin\varphi_k \sin\theta_k$, $\boldsymbol{s}_k = [s_k(1), s_k(2), \cdots, s_k(T)]^{\mathrm{T}}$ is the source signal waveform, and $\boldsymbol{\mathcal{N}}_{\mathbb{P}_i}$ is an additive Gaussian white noise tensor, i.e., $\boldsymbol{\mathcal{N}}_{\mathbb{P}_i}(:, :, t) \sim \mathcal{CN}(\boldsymbol{0}, \sigma_n^2 \boldsymbol{\mathcal{I}}), \forall t = 1, 2, \cdots, T$. Here, σ_n^2 represents the noise power, $\boldsymbol{\mathcal{I}}$ denotes the 4-D identity tensor, $\circ$ denotes the outer product, $\jmath$ denotes the imaginary unit, and $(\cdot)^{\mathrm{T}}$ denotes the transpose operator.

To calculate the second-order tensor statistics of the CPA, the 4-D cross-correlation tensor $\boldsymbol{\mathcal{R}} = \mathrm{E}\{< \boldsymbol{\mathcal{X}}_{\mathbb{P}_1} \times_3 \boldsymbol{\mathcal{X}}_{\mathbb{P}_2}^* >\}$ of $\boldsymbol{\mathcal{X}}_{\mathbb{P}_1}$ and $\boldsymbol{\mathcal{X}}_{\mathbb{P}_2}$ is calculated as

$$\boldsymbol{\mathcal{R}} = \sum_{k=1}^{K} \sigma_k^2 \boldsymbol{a}_x^{(\mathbb{P}_1)}(k) \circ \boldsymbol{a}_y^{(\mathbb{P}_1)}(k) \circ \boldsymbol{a}_x^{(\mathbb{P}_2)^*}(k) \circ \boldsymbol{a}_y^{(\mathbb{P}_2)^*}(k) + \boldsymbol{\mathcal{N}}, \quad (2)$$

where σ_k^2 represents the power of the k-th source, and $\boldsymbol{\mathcal{N}} = \mathrm{E}\{<\boldsymbol{\mathcal{N}}_{\mathbb{P}_1} \times_3 \boldsymbol{\mathcal{N}}_{\mathbb{P}_2}^* >\}$ is a noise term with only the $(1, 1, 1, 1)$-th element being σ_n^2 while all others being 0. Here, $< \cdot \times_a \cdot >$ denotes the tensor contraction operator along the a-th dimension, $\mathrm{E}\{\cdot\}$ denotes the statistical expectation operator, and $(\cdot)^*$ denotes the conjugation operator. In practice, we approximate $\boldsymbol{\mathcal{R}}$ by its sample cross-correlation tensor $\hat{\boldsymbol{\mathcal{R}}} = 1/T < \boldsymbol{\mathcal{X}}_{\mathbb{P}_1} \times_3 \boldsymbol{\mathcal{X}}_{\mathbb{P}_2}^* >$.

3. PROPOSED DOA ESTIMATION METHOD

3.1. Structured Coarray Tensor Formulation

Since the second-order statistics of sparse arrays offer a Nyquist-matched coarray signal processing [23–28], the augmented virtual array of the CPA is derived by combining the dimensions of $\boldsymbol{\mathcal{R}}$ that represent the spatial information along the same coordinate axis. Specifically, combining the dimension sets $\mathbb{S}\{1, 3\}$ and $\mathbb{S}\{2, 4\}$ of $\boldsymbol{\mathcal{R}}$, i.e., $\tilde{\boldsymbol{R}} \triangleq \boldsymbol{\mathcal{R}}_{\{1,3\}\{2,4\}} \in \mathbb{C}^{q_x^{(\mathbb{P}_1)} q_x^{(\mathbb{P}_2)} \times q_y^{(\mathbb{P}_1)} q_y^{(\mathbb{P}_2)}}$, yields

$$\tilde{\boldsymbol{R}} = \sum_{k=1}^{K} \sigma_k^2 \left[\mathbf{a}_x^{(\mathbb{P}_2)^*}(k) \otimes \mathbf{a}_x^{(\mathbb{P}_1)}(k)\right] \circ \left[\mathbf{a}_y^{(\mathbb{P}_2)^*}(k) \otimes \mathbf{a}_y^{(\mathbb{P}_1)}(k)\right], \quad (3)$$

where $\otimes$ denotes the Kronecker product. To simplify the analysis, the noise term $\boldsymbol{\mathcal{N}}$ is ignored here. As such, the reshaped cross-correlation matrix $\tilde{\boldsymbol{R}}$ corresponds to an augmented discontinuous virtual planar array $\mathbb{V}$ of size $J_x \times J_y$, where $J_x = 3M_{\mathbb{P}_1}M_{\mathbb{P}_2} - M_{\mathbb{P}_1} - M_{\mathbb{P}_2} + 1$ and $J_y = 3N_{\mathbb{P}_1}N_{\mathbb{P}_2} - N_{\mathbb{P}_1} - N_{\mathbb{P}_2} + 1$. As shown in Fig. 2(a), there are whole columns and rows of holes in $\mathbb{V}$. Although the continuous part of $\mathbb{V}$, i.e., a virtual URA $\mathbb{U}$, can be utilized for the subsequent Nyquist-matched coarray signal processing, the discarded virtual sensors $\mathbb{V} - \mathbb{U}$ will cause inevitable information loss.

To make full use of the derived virtual sensors, the discontinuous virtual planar array $\mathbb{V}$ as well as its symmetric part $\tilde{\mathbb{V}}$ are piled up to form a virtual cubic array $\mathbb{W}$. As shown in Fig. 2(b), due to the whole columns and rows of holes in $\mathbb{V}$ and $\tilde{\mathbb{V}}$, $\mathbb{W}$ also contains lateral and horizontal slices of holes. Accordingly, its corresponding 3-D incomplete coarray tensor $\boldsymbol{\mathcal{U}}_{\mathbb{W}} \in \mathbb{C}^{J_x \times J_y \times 2}$ can be constructed by reorganizing the coarray statistics in $\tilde{\boldsymbol{R}}$ and $\tilde{\boldsymbol{R}}^*$ to map the corresponding locations of virtual sensors in $\mathbb{W}$. As such, $\boldsymbol{\mathcal{U}}_{\mathbb{W}}$ can be formulated

as

$$\boldsymbol{\mathcal{U}}_{\mathbb{W}} = \sum_{k=1}^{K} \sigma_k^2 \boldsymbol{b}_x(k) \circ \boldsymbol{b}_y(k) \circ \boldsymbol{h}(k), \tag{4}$$

where $\boldsymbol{b}_x(k)$ and $\boldsymbol{b}_y(k)$ serve as the steering vectors of $\mathbb{W}$, and $\boldsymbol{h}(k)=[1, e^{-\jmath\pi\left(-(M_{\mathbb{P}_1}M_{\mathbb{P}_2}+M_{\mathbb{P}_1}+M_{\mathbb{P}_2})\mu_k-(N_{\mathbb{P}_1}N_{\mathbb{P}_2}+N_{\mathbb{P}_1}+N_{\mathbb{P}_2})\nu_k\right)}]^{\mathrm{T}}$ represents the symmetric factor for $\mathbb{V}$ and $\tilde{\mathbb{V}}$.

Although the virtual cubic array $\mathbb{W}$ did increase the virtual array aperture for DOA estimation, the slices of missing elements in $\boldsymbol{\mathcal{U}}_{\mathbb{W}}$ prevent the Nyquist-matched coarray tensor processing. Hence, it is necessary to complete $\boldsymbol{\mathcal{U}}_{\mathbb{W}}$ for Nyquist matching. However, the existing low-rank tensor completion techniques assume the locations of missing elements to be random [18, 19], indicating that all slices in the incomplete tensor cannot be entirely missing. In order to impose an effective low-rank regularization on $\boldsymbol{\mathcal{U}}_{\mathbb{W}}$ for its completion, we propose a structural tensorization approach to distribute the missing elements in $\boldsymbol{\mathcal{U}}_{\mathbb{W}}$.

To segment the whole slices of missing elements in the coarray tensor $\boldsymbol{\mathcal{U}}_{\mathbb{W}}$, we extract its elements indexed by $(u_x : u_x-1+L_x)$, $(u_y : u_y-1+L_y)$, and $(1:2)$ in the three respective dimensions to formulate $U_x \times U_y$ sub-tensors $\boldsymbol{\mathcal{U}}_{\mathbb{W}}^{(u_x,u_y)} \in \mathbb{C}^{L_x \times L_y \times 2}$, where $u_x = 1, 2, \cdots, U_x$, $u_y = 1, 2, \cdots, U_y$ with $U_x = J_x + 1 - L_x$ and $U_y = J_y + 1 - L_y$, and $2 \leqslant L_x \leqslant J_x - 1$, $2 \leqslant L_y \leqslant J_y - 1$. Since these sub-tensors own a shifting invariance relationship with each other, they are concatenated to generate two additional shifting dimensions upon the original three spatial dimensions, such that the missing elements can be distributed into all five dimensions. Specifically, the sub-tensors $\boldsymbol{\mathcal{U}}_{\mathbb{W}}^{(u_x,u_y)}$ with the same index u_y are concatenated in the fourth dimension, and the resulting U_y 4-D tensors of size $L_x \times L_y \times 2 \times U_x$ are further concatenated to formulate a 5-D incomplete coarray tensor $\boldsymbol{\mathcal{T}}_{\mathbb{W}} \in \mathbb{C}^{L_x \times L_y \times 2 \times U_x \times U_y}$. Let dimension sets $\mathbb{S}\{1, 2\}$, $\mathbb{S}\{4, 5\}$ and $\mathbb{S}\{3\}$ respectively represent the angular information, shifting information and symmetric information, $\boldsymbol{\mathcal{T}}_{\mathbb{W}}$ can be structurally reshaped into a 3-D incomplete coarray tensor $\boldsymbol{\mathcal{D}}_{\mathbb{W}} \triangleq \boldsymbol{\mathcal{T}}_{\mathbb{W}\{1,2\},\{4,5\},\{3\}} \in \mathbb{C}^{L_x L_y \times U_x U_y \times 2}$ whose missing elements are distributed.

3.2. Coarray Tensor Completion for DOA Estimation

For the incomplete coarray tensor $\boldsymbol{\mathcal{D}}_{\mathbb{W}}$ with distributed missing elements, the low-rank regularization can be applied for coarray tensor completion. Hence, a tensor nuclear norm minimization problem can be formulated as

$$\begin{aligned} \min_{\bar{\boldsymbol{\mathcal{D}}}_{\bar{\mathbb{W}}}} \ & \|\bar{\boldsymbol{\mathcal{D}}}_{\bar{\mathbb{W}}}\|_* \\ \text{s.t.} \ & \mathcal{P}_{\Omega}(\bar{\boldsymbol{\mathcal{D}}}_{\bar{\mathbb{W}}}) = \mathcal{P}_{\Omega}(\boldsymbol{\mathcal{D}}_{\mathbb{W}}), \end{aligned} \tag{5}$$

where the optimization variable $\bar{\boldsymbol{\mathcal{D}}}_{\bar{\mathbb{W}}}$ is the completed coarray tensor corresponding to the filled virtual cubic array $\bar{\mathbb{W}}$, Ω is the index set of the non-zero elements in $\boldsymbol{\mathcal{D}}_{\mathbb{W}}$, $\|\cdot\|_*$ denotes the nuclear norm, and $\mathcal{P}_{\Omega}(\cdot)$ denotes the projection operator on Ω. The optimization problem (5) is convex because the nuclear norm of the completed coarray tensor $\bar{\boldsymbol{\mathcal{D}}}_{\bar{\mathbb{W}}}$ is a convex combination of the nuclear norms of its three unfoldings, i.e., $\|\bar{\boldsymbol{\mathcal{D}}}_{\bar{\mathbb{W}}}\|_* = \sum_{b=1}^{3} \alpha_b \|\bar{\boldsymbol{\mathcal{D}}}_{\bar{\mathbb{W}}}(b)\|_*$. Here, $\bar{\boldsymbol{\mathcal{D}}}_{\bar{\mathbb{W}}}(b)$ denotes the mode-b unfolding of $\bar{\boldsymbol{\mathcal{D}}}_{\bar{\mathbb{W}}}$, $b = 1, 2, 3$, and $\alpha_b \geqslant 0$ is the corresponding coefficient satisfying $\sum_{b=1}^{3} \alpha_b = 1$. Nonetheless, these coarray tensor nuclear norms $\|\bar{\boldsymbol{\mathcal{D}}}_{\bar{\mathbb{W}}}(b)\|_*$ are nonsmooth, which causes a low convergence rate to solve (5) using the interior point method.

Since the alternating direction method of multipliers (ADMM) presents an optimal convergence performance in solving optimization problems with nonsmooth terms in the objective [29], we utilize the ADMM framework to solve (5). In particular, to ensure the three constituting nuclear norms $\|\bar{\boldsymbol{\mathcal{D}}}_{\bar{\mathbb{W}}}(1)\|_*$, $\|\bar{\boldsymbol{\mathcal{D}}}_{\bar{\mathbb{W}}}(2)\|_*$ and $\|\bar{\boldsymbol{\mathcal{D}}}_{\bar{\mathbb{W}}}(3)\|_*$ in the objective of (5) are independent to each other, the auxiliary tensors $\boldsymbol{\mathcal{Y}}_b = \bar{\boldsymbol{\mathcal{D}}}_{\bar{\mathbb{W}}}$, $b = 1, 2, 3$, are introduced to convert (5) into

$$\begin{aligned} \min_{\bar{\boldsymbol{\mathcal{D}}}_{\bar{\mathbb{W}}}, \boldsymbol{\mathcal{Y}}_1, \boldsymbol{\mathcal{Y}}_2, \boldsymbol{\mathcal{Y}}_3} \ & \|\bar{\boldsymbol{\mathcal{D}}}_{\bar{\mathbb{W}}}\|_* \\ \text{s.t.} \ & \mathcal{P}_{\Omega}(\bar{\boldsymbol{\mathcal{D}}}_{\bar{\mathbb{W}}}) = \mathcal{P}_{\Omega}(\boldsymbol{\mathcal{D}}_{\mathbb{W}}), \\ & \bar{\boldsymbol{\mathcal{D}}}_{\bar{\mathbb{W}}} - \boldsymbol{\mathcal{Y}}_b = \boldsymbol{0}. \end{aligned} \tag{6}$$

Then, by introducing dual variables $\boldsymbol{\mathcal{M}}_b \in \mathbb{C}^{L_x L_y \times U_x U_y \times 2}$ of $\bar{\boldsymbol{\mathcal{D}}}_{\bar{\mathbb{W}}}$, the augmented Lagrangian function is defined as

$$\begin{aligned} &\Gamma(\bar{\boldsymbol{\mathcal{D}}}_{\bar{\mathbb{W}}}, \boldsymbol{\mathcal{Y}}_1, \boldsymbol{\mathcal{Y}}_2, \boldsymbol{\mathcal{Y}}_3, \boldsymbol{\mathcal{M}}_1, \boldsymbol{\mathcal{M}}_2, \boldsymbol{\mathcal{M}}_3) \\ &= \|\bar{\boldsymbol{\mathcal{D}}}_{\bar{\mathbb{W}}}\|_* + [(\bar{\boldsymbol{\mathcal{D}}}_{\bar{\mathbb{W}}} - \boldsymbol{\mathcal{Y}}_b) \times \boldsymbol{\mathcal{M}}_b] + \frac{\rho}{2} \|\bar{\boldsymbol{\mathcal{D}}}_{\bar{\mathbb{W}}} - \boldsymbol{\mathcal{Y}}_b\|_{\mathrm{F}}^2, \end{aligned} \tag{7}$$

where ρ is the penalty constant, $[\,\times\,]$ denotes the tensor inner product, and $\|\cdot\|_{\mathrm{F}}$ denotes the Frobenius norm. Here, $\bar{\boldsymbol{\mathcal{D}}}_{\bar{\mathbb{W}}}$, $\boldsymbol{\mathcal{Y}}_b$ and $\boldsymbol{\mathcal{M}}_b$ at the $(\eta+1)$-th iteration can be updated as

$$\begin{aligned} \boldsymbol{\mathcal{Y}}_b^{(\eta+1)} &= \operatorname*{argmin}_{\boldsymbol{\mathcal{Y}}_b} \Gamma\big(\bar{\boldsymbol{\mathcal{D}}}_{\bar{\mathbb{W}}}^{(\eta)}, \boldsymbol{\mathcal{Y}}_b, \boldsymbol{\mathcal{M}}_b^{(\eta)}\big), \\ \bar{\boldsymbol{\mathcal{D}}}_{\bar{\mathbb{W}}}^{(\eta+1)} &= \operatorname*{argmin}_{\bar{\boldsymbol{\mathcal{D}}}_{\bar{\mathbb{W}}}} \Gamma\big(\bar{\boldsymbol{\mathcal{D}}}_{\bar{\mathbb{W}}}, \boldsymbol{\mathcal{Y}}_b^{(\eta+1)}, \boldsymbol{\mathcal{M}}_b^{(\eta)}\big), \\ \boldsymbol{\mathcal{M}}_b^{(\eta+1)} &= \boldsymbol{\mathcal{M}}_b^{(\eta)} - \rho\big(\boldsymbol{\mathcal{Y}}_b^{(\eta+1)} - \bar{\boldsymbol{\mathcal{D}}}_{\bar{\mathbb{W}}}^{(\eta+1)}\big). \end{aligned} \tag{8}$$

The iteration converges when the difference between $\bar{\boldsymbol{\mathcal{D}}}_{\bar{\mathbb{W}}}^{(\eta+1)}$ and $\bar{\boldsymbol{\mathcal{D}}}_{\bar{\mathbb{W}}}^{(\eta)}$ is smaller than a tolerance ϵ.

To retrieve the angle information from the completed coarray tensor $\bar{\boldsymbol{\mathcal{D}}}_{\bar{\mathbb{W}}}$ for DOA estimation, the outer product expression for the completed version of the 5-D tensor $\boldsymbol{\mathcal{T}}_{\mathbb{W}}$, i.e., $\bar{\boldsymbol{\mathcal{T}}}_{\bar{\mathbb{W}}}$, is investigated. Since the outer product expression of the completed coarray tensor $\bar{\boldsymbol{\mathcal{U}}}_{\bar{\mathbb{W}}}$ contains the steering vectors $\bar{\boldsymbol{b}}_x(k) = [e^{-\jmath\pi(-M_{\mathbb{P}_1}M_{\mathbb{P}_2}+M_{\mathbb{P}_1})\mu_k}, e^{-\jmath\pi(-M_{\mathbb{P}_1}M_{\mathbb{P}_2}+M_{\mathbb{P}_1}+1)\mu_k}, \cdots, e^{-\jmath\pi(2M_{\mathbb{P}_1}M_{\mathbb{P}_2}-M_{\mathbb{P}_2})\mu_k}]^{\mathrm{T}}$ and $\bar{\boldsymbol{b}}_y(k) = [e^{-\jmath\pi(-N_{\mathbb{P}_1}N_{\mathbb{P}_2}+N_{\mathbb{P}_1})\nu_k}, e^{-\jmath\pi(-N_{\mathbb{P}_1}N_{\mathbb{P}_2}+N_{\mathbb{P}_1}+1)\nu_k}, \cdots, e^{-\jmath\pi(2N_{\mathbb{P}_1}N_{\mathbb{P}_2}-N_{\mathbb{P}_2})\nu_k}]^{\mathrm{T}}$ of the filled virtual cubic array $\bar{\mathbb{W}}$, $\bar{\boldsymbol{\mathcal{T}}}_{\bar{\mathbb{W}}}$ can be generated from $\bar{\boldsymbol{\mathcal{U}}}_{\bar{\mathbb{W}}}$ as

$$\bar{\boldsymbol{\mathcal{T}}}_{\bar{\mathbb{W}}} = \sum_{k=1}^{K} \sigma_k^2 \tilde{\boldsymbol{b}}_x(k) \circ \tilde{\boldsymbol{b}}_y(k) \circ \boldsymbol{h}(k) \circ \boldsymbol{u}_x(k) \circ \boldsymbol{u}_y(k) \tag{9}$$

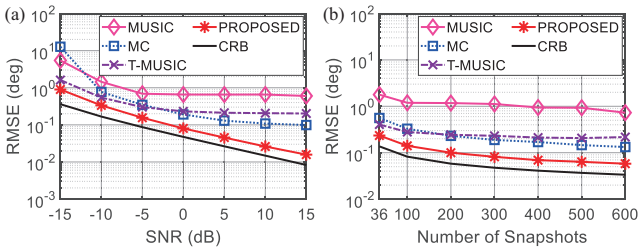

Fig. 3. Estimation accuracy comparison. (a) RMSE versus SNR, $T=300$; (b) RMSE versus snapshots, SNR$=0$ dB.

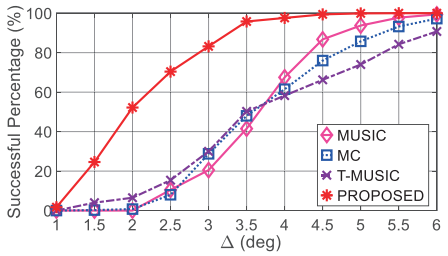

Fig. 4. Resolution comparison. SNR $=0$ dB, $T=300$.

through the sub-tensor concatenation operation as in Section 3.1. Here, $\tilde{\boldsymbol{b}}_x(k)$ consists of the first L_x-th elements in $\bar{\boldsymbol{b}}_x(k)$, $\tilde{\boldsymbol{b}}_y(k)$ consists of the first L_y-th elements in $\bar{\boldsymbol{b}}_y(k)$, and $\boldsymbol{u}_x(k)=[1,e^{-\jmath\pi\mu_k},\cdots,e^{-\jmath\pi(U_x-1)\mu_k}]^{\mathrm{T}}$, $\boldsymbol{u}_y(k)=[1,e^{-\jmath\pi\nu_k},\cdots,e^{-\jmath\pi(U_y-1)\nu_k}]^{\mathrm{T}}$ are the shifting factors along the x,y-axes, respectively. Then, following the structural tensorization process as in Section 3.1, the completed coarray tensor $\bar{\boldsymbol{\mathcal{D}}}_{\bar{\mathbb{W}}}$ can be modeled as

$$\bar{\boldsymbol{\mathcal{D}}}_{\bar{\mathbb{W}}}\triangleq\bar{\boldsymbol{\mathcal{T}}}_{\bar{\mathbb{W}}_{\{1,2\},\{4,5\},\{3\}}}=\sum_{k=1}^{K}\sigma_k^2\boldsymbol{g}(k)\circ\boldsymbol{l}(k)\circ\boldsymbol{h}(k),\quad(10)$$

where $\boldsymbol{g}(k)=\tilde{\boldsymbol{b}}_y(k)\otimes\tilde{\boldsymbol{b}}_x(k)$, $\boldsymbol{l}(k)=\boldsymbol{u}_y(k)\otimes\boldsymbol{u}_x(k)$ are the angular factor and shifting factor of $\bar{\boldsymbol{\mathcal{D}}}_{\bar{\mathbb{W}}}$, respectively.

Finally, applying the canonical polyadic decomposition (CPD) on $\bar{\boldsymbol{\mathcal{D}}}_{\bar{\mathbb{W}}}$ yields the estimated factors $\hat{\boldsymbol{g}}(k)$, $\hat{\boldsymbol{l}}(k)$, and $\hat{\boldsymbol{h}}(k)$, which can be utilized to calculate the parameters

$$\begin{aligned}\hat{\mu}_k&=\big[\angle(\hat{\boldsymbol{g}}_{(\zeta_1+1)}(k)/\hat{\boldsymbol{g}}_{(\zeta_1)}(k))+\angle(\hat{\boldsymbol{l}}_{(\zeta_2+1)}(k)/\hat{\boldsymbol{l}}_{(\zeta_2)}(k))\big]/2\pi,\\ \hat{\nu}_k&=\big[\angle(\hat{\boldsymbol{g}}_{(L_x+\delta_1)}(k)/\hat{\boldsymbol{g}}_{(\delta_1)}(k))+\angle(\hat{\boldsymbol{l}}_{(U_x+\delta_2)}(k)/\hat{\boldsymbol{l}}_{(\delta_2)}(k))\big]/2\pi.\end{aligned}\quad(11)$$

Here, $\angle(\cdot)$ denotes the phase of a complex number, and $\boldsymbol{a}_{(j)}$ denotes the j-th element of a vector $\boldsymbol{a}$. Based on the Kronecker structure of $\boldsymbol{g}(k)$ and $\boldsymbol{l}(k)$, $\zeta_1\in[1,L_xL_y-1]$ and $\zeta_2\in[1,U_xU_y-1]$ satisfy $\mathrm{mod}(\zeta_1,L_y)\neq0$ and $\mathrm{mod}(\zeta_2,U_y)\neq0$, respectively, and $\delta_1\in[1,L_xL_y-L_x]$, $\delta_2\in[1,U_xU_y-U_x]$, where $\mathrm{mod}(\cdot)$ denotes the modulo operator. According to the relationship between (θ_k,φ_k) and (μ_k,ν_k) established in Section 2, the DOA of the k-th source can be estimated as

$$\hat{\theta}_k=\arctan(\hat{\nu}_k/\hat{\mu}_k),\ \hat{\varphi}_k=\arcsin\left(\sqrt{\hat{\mu}_k^2+\hat{\nu}_k^2}\right).\quad(12)$$

4. SIMULATION RESULTS

In the simulations, we consider a CPA with $M_{\mathbb{P}_1}=2$, $N_{\mathbb{P}_1}=3$, $M_{\mathbb{P}_2}=3$, and $N_{\mathbb{P}_2}=4$. Hence, the total number of sensors is 35. According to the range of the sub-tensors' size as discussed in Section 3.1, it is selected as $(L_x,L_y)=(6,11)$. The penalty constant of the ADMM is set to $\rho=10^{-3}$, and the tolerance ϵ for the coarray tensor completion problem is set to 10^{-6}. The proposed method is compared to competing methods including the MUSIC-based method [30], the matrix completion (MC)-based method [14], and the coarray-based tensor MUSIC (T-MUSIC) method [7]. In addition, the Cramér-Rao bound for DOA estimation with the coprime planar array [15, 31, 32] is presented as the reference.

The DOA estimation accuracy of the tested methods is compared in Fig. 3, where two sources are respectively located at $(30.6°,25.6°)$ and $(40.5°,50.5°)$. The root mean square error (RMSE) is adopted as the evaluation metric, and $1,000$ Monte-Carlo trials are run for each scenario. The DOA estimation accuracy of the proposed method outperforms both MUSIC and tensor MUSIC methods because it makes full use of the discontinuous virtual array $\mathbb{W}$, whereas the other methods only consider its continuous part $\mathbb{U}$. Moreover, due to the utilization of the structural coarray tensor statistics, the proposed method demonstrates a prominent advantage over the competing matrix completion-based method.

In Fig. 4, the resolution of the tested methods is compared by considering two closely placed sources (θ_1,φ_1) and (θ_2,φ_2). Here, both θ_1 and φ_1 are randomly selected between $[20°,30°]$ for each trial. θ_2 has an angular spacing of Δ with θ_1, i.e., $(\theta_2,\varphi_2)=(\theta_1+\Delta,\varphi_1)$ for the first $1,000$ trials, whereas φ_2 has the same angular spacing of Δ with φ_1, i.e., $(\theta_2,\varphi_2)=(\theta_1,\varphi_1+\Delta)$ for the next $1,000$ trials. The tested method is identified to successfully estimate the DOAs if $|\hat{\theta}_k-\theta_k|<\Delta/2$ and $|\hat{\varphi}_k-\varphi_k|<\Delta/2$ for each trial. It is clear that the proposed method has the highest successful percentage among the tested methods. These results confirm that the proposed method effectively exploits the entire coarray tensor statistics, leading to an enhanced resolution.

5. CONCLUSION

In this paper, we proposed a coarray tensor completion-based DOA estimation method for coprime planar array, where the missing slices of the coarray tensor are completed. The whole slices of missing elements in the coarray tensor are distributed via structural tensorization. As such, the structured coarray tensor can be completed with a low-rank regularization. Simulation results corroborate the superior performance of the proposed method compared to competing methods.

6. REFERENCES

[1] P. P. Vaidyanathan and P. Pal, "Sparse sensing with co-prime samplers and arrays," *IEEE Trans. Signal Process.*, vol. 59, no. 2, pp. 573–586, Feb. 2011.

[2] C. Zhou, Y. Gu, S. He, and Z. Shi, "A robust and efficient algorithm for coprime array adaptive beamforming," *IEEE Trans. Veh. Technol.*, vol. 67, no. 2, pp. 1099–1112, Feb. 2018.

[3] X. Wu and W.-P. Zhu, "Single far-field or near-field source localization with sparse or uniform cross array," *IEEE Trans. Veh. Technol.*, vol. 69, no. 8, pp. 9135–9139, Aug. 2020.

[4] C. Zhou, Y. Gu, Z. Shi, and Y. D. Zhang, "Off-grid direction-of-arrival estimation using coprime array interpolation," *IEEE Signal Process. Lett.*, vol. 25, no. 11, pp. 1710–1714, Nov. 2018.

[5] Y. Gu and A. Leshem, "Robust adaptive beamforming based on interference covariance matrix reconstruction and steering vector estimation," *IEEE Trans. Signal Process.*, vol. 60, no. 7, pp. 3881–3885, July 2012.

[6] C. Zhou, Z. Shi, Y. Gu, and X. Shen, "DECOM: DOA estimation with combined MUSIC for coprime array," in *Proc. WCSP*, Hangzhou, China, Oct. 2013, pp. 1–5.

[7] C.-L. Liu and P. P. Vaidyanathan, "Tensor MUSIC in multidimensional sparse arrays," in *Proc. ACSSC*, Pacific Grove, CA, Nov. 2015, pp. 1783–1787.

[8] C. Shi, Y. Wang, S. Salous, J. Zhou, and J. Yan, "Joint transmit resource management and waveform selection strategy for target tracking in distributed phased array radar network," *IEEE Trans. Aerosp. Electron. Syst.*, DOI: 10.1109/TAES.2021.3138869.

[9] H. Zheng, Z. Shi, C. Zhou, M. Haardt, and J. Chen, "Coupled coarray tensor CPD for DOA estimation with coprime L-shaped array," *IEEE Signal Process. Lett.*, vol. 28, pp. 1545–1549, July 2021.

[10] J. Shi, D. Wu, and Z. Li, "Tensor-based angle estimation with coprime MIMO radar," in *Proc. IEEE SAM*, Hangzhou, China, June 2020, pp. 1–4.

[11] H. Zheng, C. Zhou, Y. Wang, and Z. Shi, "2-D DOA estimation for coprime cubic array: A cross-correlation tensor perspective," in *Proc. ISAP*, Osaka, Japan, Jan. 2021, pp. 447–448.

[12] C. Zhou, H. Zheng, Y. Gu, Y. Wang, and Z. Shi, "Research progress on coprime array signal processing: Direction-of-arrival estimation and adaptive beamforming," *Journal of Radars*, vol. 8, no. 5, pp. 558–577, Oct. 2019.

[13] C. Zhou, Y. Gu, Z. Shi, and M. Haardt, "Direction-of-arrival estimation for coprime arrays via coarray correlation reconstruction: A one-bit perspective," in *Proc. IEEE SAM*, Hangzhou, China, June 2020, pp. 1–4.

[14] C.-L. Liu, P. P. Vaidyanathan, and P. Pal, "Coprime coarray interpolation for DOA estimation via nuclear norm minimization," in *Proc. IEEE ISCAS*, Montréal, Canada, May 2016, pp. 2639–2642.

[15] C. Zhou, Y. Gu, X. Fan, Z. Shi, G. Mao, and Y. D. Zhang, "Direction-of-arrival estimation for coprime array via virtual array interpolation," *IEEE Trans. Signal Process.*, vol. 66, no. 22, pp. 5956–5971, Nov. 2018.

[16] X. Fan, C. Zhou, Y. Gu, and Z. Shi, "Toeplitz matrix reconstruction of interpolated coprime virtual array for DOA estimation," in *Proc. IEEE VTC-Spring*, Sydney, Australia, June 2017.

[17] H. Qiao and P. Pal, "Unified analysis of co-array interpolation for direction-of-arrival estimation," in *Proc. IEEE ICASSP*, New Orleans, LA, Mar. 2017, pp. 3056–3060.

[18] J. Liu, P. Musialski, P. Wonka, and J. Ye, "Tensor completion for estimating missing values in visual data," *IEEE Trans. Pattern Anal. Mach. Intell.*, vol. 35, no. 1, pp. 208–220, Jan. 2013.

[19] M. S. Asif and A. Prater-Bennette, "Low-rank tensor ring model for completing missing visual data," in *Proc. IEEE ICASSP*, Barcelona, Spain, May 2020, pp. 5415–5419.

[20] H. Zheng, C. Zhou, Y. Gu, and Z. Shi, "Two-dimensional DOA estimation for coprime planar array: A coarray tensor-based solution," in *Proc. IEEE ICASSP*, Barcelona, Spain, May 2020, pp. 4562–4566.

[21] T. Yokota, B. Erem, S. Guler, S. K. Warfield, and H. Hontani, "Missing slice recovery for tensors using a low-rank model in embedded space," in *Proc. IEEE CVPR*, Salt Lake City, UT, June 2018, pp. 8251–8259.

[22] F. Sedighin, A. Cichocki, T. Yokota, and Q. Shi, "Matrix and tensor completion in multiway delay embedded space using tensor train, with application to signal reconstruction," *IEEE Signal Process. Lett.*, vol. 27, pp. 810–814, Apr. 2020.

[23] C. Zhou, Y. Gu, Y. D. Zhang, Z. Shi, T. Jin, and X. Wu, "Compressive sensing-based coprime array direction-of-arrival estimation," *IET Commun.*, vol. 11, pp. 1719–1724, Aug. 2017.

[24] X. Wu, "Localization of far-field and near-field signals with mixed sparse approach: A generalized symmetric arrays perspective," *Signal Process.*, vol. 175, pp. 107665, Oct. 2020.

[25] Z. Shi, C. Zhou, Y. Gu, N. A. Goodman, and F. Qu, "Source estimation using coprime array: A sparse reconstruction perspective," *IEEE Sensors J.*, vol. 17, pp. 755–765, Feb. 2017.

[26] J. Li, P. Ma, X. Zhang, and G. Zhao, "Improved DFT algorithm for 2D DOA estimation based on 1D nested array motion," *IEEE Commun. Lett.*, vol. 24, no. 9, pp. 1953–1956, Sept. 2020.

[27] Y. Shen, C. Zhou, Y. Gu, H. Lin, and Z. Shi, "Vandermonde decomposition of coprime coarray covariance matrix for DOA estimation," in *Proc. SPAWC*, Sapporo, Japan, July 2017.

[28] F. Zhu, J. Gao, J. Yang, and N. Ye, "Neighborhood linear discriminant analysis," *Pattern Recognit.*, vol. 123, pp. 108422, Mar. 2022.

[29] Z. Lin, M. Chen, and Y. Ma, *The Augmented Lagrange Multiplier Method for Exact Recovery of Corrupted Low-Rank Matrices*, Technical Report UILU-ENG-09-2215, Nov. 2009.

[30] W. Zheng, X. Zhang, and H. Zhai, "Generalized coprime planar array geometry for 2-D DOA estimation," *IEEE Commun. Lett.*, vol. 21, no. 5, pp. 1075–1078, May 2017.

[31] C.-L. Liu and P. P. Vaidyanathan, "Cramér-Rao bounds for coprime and other sparse arrays, which find more sources than sensors," *Digit. Signal Process.*, vol. 61, pp. 43–61, Feb. 2017.

[32] M. Wang and A. Nehorai, "Coarrays, MUSIC, and the Cramér-Rao bound," *IEEE Trans. Signal Process.*, vol. 65, no. 4, pp. 933–946, Feb. 2017.